 Related Commentary, page 2090

Proteinuria precedes podocyte abnormalities in *Lamb2*$^{-/-}$ mice, implicating the glomerular basement membrane as an albumin barrier

George Jarad,[1] Jeanette Cunningham,[1] Andrey S. Shaw,[2] and Jeffrey H. Miner[1]

[1]Renal Division, Department of Internal Medicine, and [2]Department of Pathology and Immunology, Washington University School of Medicine, St. Louis, Missouri, USA.

Primary defects in either podocytes or the glomerular basement membrane (GBM) cause proteinuria, a fact that complicates defining the barrier to albumin. Laminin β2 (LAMB2) is a GBM component required for proper functioning of the glomerular filtration barrier. To investigate the GBM's role in glomerular filtration, we characterized GBM and overlying podocyte architecture in relation to development and progression of proteinuria in *Lamb2*$^{-/-}$ mice, which model Pierson syndrome, a rare congenital nephrotic syndrome. We found ectopic deposition of several laminins and mislocalization of anionic sites in the GBM, which together suggest that the *Lamb2*$^{-/-}$ GBM is severely disorganized, although it is ultrastructurally intact. Importantly, albuminuria was detectable shortly after birth and preceded podocyte foot process effacement and loss of slit diaphragms by at least 7 days. Expression and localization of slit diaphragm and foot process–associated proteins appeared normal at early stages. GBM permeability to the electron-dense tracer ferritin was dramatically elevated in *Lamb2*$^{-/-}$ mice, even before widespread foot process effacement. Increased ferritin permeability was not observed in nephrotic CD2-associated protein–null (*Cd2ap*$^{-/-}$) mice, which have a primary podocyte defect. Together these data show that the GBM serves as a barrier to protein in vivo and that the glomerular slit diaphragm alone is not sufficient to prevent the passage of albumin into the urinary space.

Introduction

Laminins are heterotrimeric basement membrane (BM) glycoproteins consisting of α, β, and γ chains. In mammals there are 5 α, 4 β, and 3 γ chains that assemble to form at least 15 heterotrimers (1). Laminins provide the basic scaffold for assembly of other BM components, including type IV collagen, nidogen/entactin, and sulfated proteoglycans (2). BMs are the thin sheets of extracellular matrix adjacent to many cell types, including most epithelia and endothelia. Their importance extends beyond merely providing mechanical support for cells; BMs are critical for cell proliferation, differentiation, survival, and function, as has been clearly shown in human diseases or animal models with BM abnormalities (1, 3).

The kidney glomerular BM (GBM) is an unusually thick BM formed via fusion of distinct BMs assembled by glomerular epithelial cells (podocytes) and glomerular endothelial cells (4). The GBM is functionally unique; it must facilitate constant fluid flow across the glomerular filtration barrier (GFB) — consisting of endothelium, GBM, and podocyte — while tolerating hemodynamic stresses and providing support for glomerular cells. The composition of the GBM is also specialized, as it is the only nephron-associated BM in the kidney whose laminin composition is exclusively laminin α5β2γ1, referred to as LM-521 in the new nomenclature (3, 5).

Whereas the α5 chain, as part of LM-511 (α5β1γ1) and LM-521, is required for GBM integrity and glomerular vascularization (6), the β2 chain is dispensable for glomerulogenesis. Laminin β2–null (*Lamb2*$^{-/-}$) mice are born alive overtly indistinguishable from normal littermates (7, 8). GBM ultrastructure appears essentially normal, because LM-511, normally found in immature GBM, compensates structurally for the missing LM-521 in mature GBM (8). *Lamb2*$^{-/-}$ mice develop severe neuromuscular defects and nephrotic syndrome with progressive foot process (FP) effacement. Mutant mice fail to thrive; they stop gaining weight at P7 and die at approximately P21 due primarily to the neuromuscular defects (9). The mouse *Lamb2*$^{-/-}$ phenotype shows similarities to Pierson syndrome, a recently described human disease resulting from *LAMB2* mutations and characterized by ocular abnormalities, psychomotor defects, and congenital nephrotic syndrome (10).

The cardinal feature of nephrotic syndrome is severe proteinuria resulting from increased flux of albumin and other plasma proteins across the GFB. The GBM's role in glomerular permselectivity, if any, is not clear, and it is now considered secondary to that of the podocyte slit diaphragm (SD) (11, 12). Nevertheless, proteinuria can result from either primary podocyte or primary GBM defects, so how a GBM compositional or structural defect might cause proteinuria is still debated. Some investigators have suggested podocyte detachment from the GBM as a possible explanation (13), and this was supported in some kidney injury models by the presence of viable podocytes in urine (14). However, in the absence of an acute, severe injury, it is rare to find denuded GBM. Another possibility is that abnormal matrix components signal anomalously via podocyte cell surface receptors and disrupt podocyte homeostasis, but this has not been addressed in vivo. The last theory is that the GBM is a major factor in determining glomerular permselectivity by acting as a modified gel through which macromolecules such as albumin pass primarily by diffusion, indepen-

Nonstandard abbreviations used: *Cd2ap*$^{-/-}$, CD2-associated protein–null; BM, basement membrane; FP, foot process; GBM, glomerular BM; GFB, glomerular filtration barrier; *Lamb2*$^{-/-}$, laminin β2–null; SD, slit diaphragm; SEM, scanning electron microscopy; TEM, transmission electron microscopy.

Conflict of interest: The authors have declared that no conflict of interest exists.

Citation for this article: *J. Clin. Invest.* **116**:2272–2279 (2006). doi:10.1172/JCI28414.

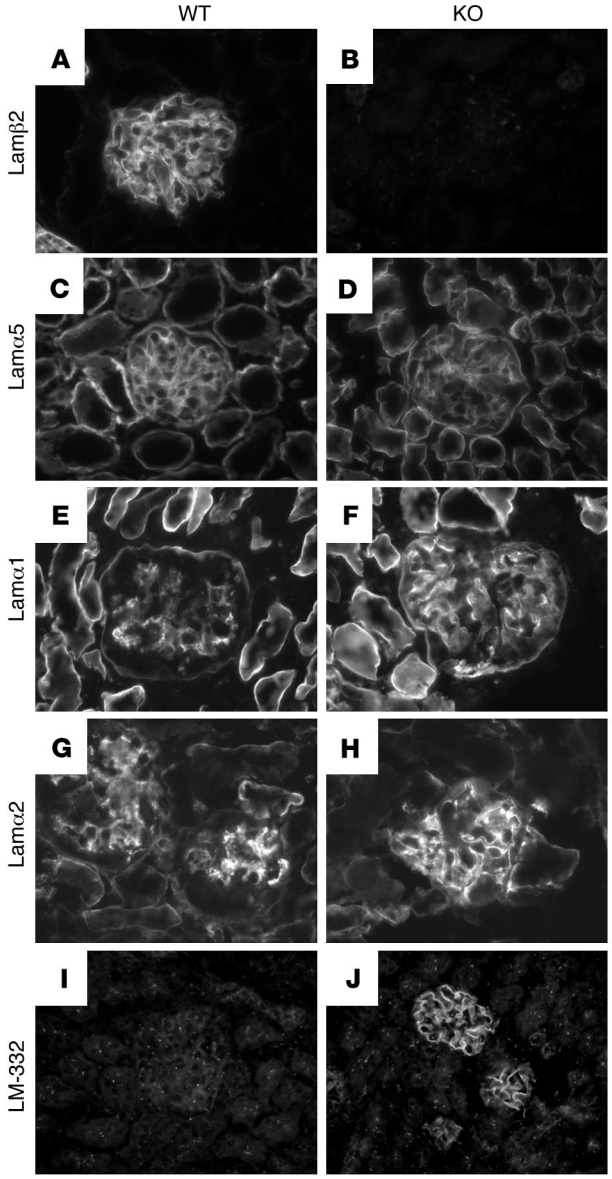

Figure 1
Immunofluorescence detection of glomerular laminins. Frozen sections of normal (left) and *Lamb2*$^{-/-}$ (right) kidneys were stained for laminin β2 (Lamβ2; **A** and **B**), α5 (**C** and **D**), α1 (**E** and **F**), α2 (**G** and **H**), and α3β3γ2 (LM-332; **I** and **J**). Normal GBM contains laminin β2 and α5 (and γ1; data not shown); laminin α5 was decreased in *Lamb2*$^{-/-}$ GBM. Normal glomeruli exhibit variable mesangial staining for laminin α1 and α2 but not LM-332; however, all were detected ectopically in *Lamb2*$^{-/-}$ GBM. Original magnification, ×600.

dent of fluid flow (the gel permeation/diffusion hypothesis; ref. 15). In this model, an increased protein concentration in the glomerular ultrafiltrate can result from either of 2 mechanisms: (a) an alteration in the composition of the GBM, as occurs in Pierson syndrome and Alport syndrome (16, 17); or (b) a reduction in the rate of fluid flow across the GFB, as is proposed to occur in cases of FP effacement due to reduced filtration slit frequency, without change in the rate of protein diffusion (15).

Tubules also play an important role in proteinuria, as the concentration of protein in the final urine is determined not only by the GFB but also by tubular reabsorption of filtered protein. Previous work using isolated proximal tubules suggests that albumin uptake is biphasic; there is a high-affinity/low-capacity pathway that is saturable at physiologic albumin concentrations and a low-affinity/high-capacity pathway associated with bulk fluid uptake (18). This underscores the importance of albumin concentration in the glomerular filtrate rather than the absolute amount, a concept invoked by the gel permeation/diffusion hypothesis (15).

Here we investigated the compositional, structural, and functional changes in the GBM of *Lamb2*$^{-/-}$ mice and the pathophysiological consequences. This study was aided by the development of separate transgene-mediated rescues of the neuromuscular and glomerular components of the failure-to-thrive phenotype (9). *Lamb2*$^{-/-}$ mice carrying a muscle-specific β2 transgene gain weight normally and only exhibit the glomerular defect. Thus, our analyses of the GFB in older nephrotic mice are not subject to potentially confounding extrarenal defects. Using the electron-dense tracer ferritin, we were able to test the gel permeation hypothesis and identify mechanistic differences in permselectivity defects between the *Lamb2*$^{-/-}$ (GBM defect) and CD2-associated protein–null (*Cd2ap*$^{-/-}$) (podocyte defect) models of nephrotic syndrome. Our results show that the GBM has intrinsic and mutable barrier properties in response to ferritin in vivo, independent of FP architecture, and we conclude that the same is likely true for albumin.

Results

Lamb2$^{-/-}$ mice exhibit a failure-to-thrive phenotype with severe neuromuscular weakness and congenital nephrotic syndrome (7, 8), features consistent with human Pierson syndrome (10). In order to study these defects independently, we generated transgenic mice expressing rat laminin β2 either in muscle (using the muscle creatine kinase promoter; MCK-B2 transgene) or in podocytes (using the nephrin promoter; NEPH-B2 transgene). When bred onto the *Lamb2*$^{-/-}$ background, MCK-B2 rescues the neuromuscular junction defects, and NEPH-B2 prevents nephrotic syndrome (9). Although rescue of muscle has no effect on proteinuria, *Lamb2*$^{-/-}$MCK-B2 mice are overall much healthier than *Lamb2*$^{-/-}$ mice. Nevertheless, *Lamb2*$^{-/-}$MCK-B2 mice die at 1 month of age from nephrotic syndrome (9) with elevated blood urea nitrogen levels (data not shown). Here, we took advantage of the improved health and weight gain of *Lamb2*$^{-/-}$MCK-B2 mice to study the isolated GFB defect in more detail.

GBM composition and podocyte laminin receptors. During glomerular maturation, a developmental shift in the laminin components of the GBM occurs, from LM-111 to LM-511 to LM-521 (19). In the absence of laminin β2, laminin β1 persists in the GBM (8). Similarly, in Alport syndrome there is reexpression of fetal laminins α1 and β1 (16, 20), suggesting the possible existence of a compensatory response to abnormal GBM. We further investigated GBM laminin content in *Lamb2*$^{-/-}$ mice. Laminin α5 was present in the GBM regardless of whether laminin β2 was present, but levels were reduced in *Lamb2*$^{-/-}$ GBM (Figure 1, A–D). In normal kidneys the GBM lacked laminin α1 and α2 and LM-332 (Figure 1, E, G, and I), whereas *Lamb2*$^{-/-}$ GBM exhibited linear staining for all these laminins (Figure 1, F, H, and J). Together with the presence of proteinuria, these results suggest that ectopic laminins are not sufficient to restore GFB function, and their deposition in the GBM may even be pathogenic, as proposed for ectopic laminins in Alport syndrome

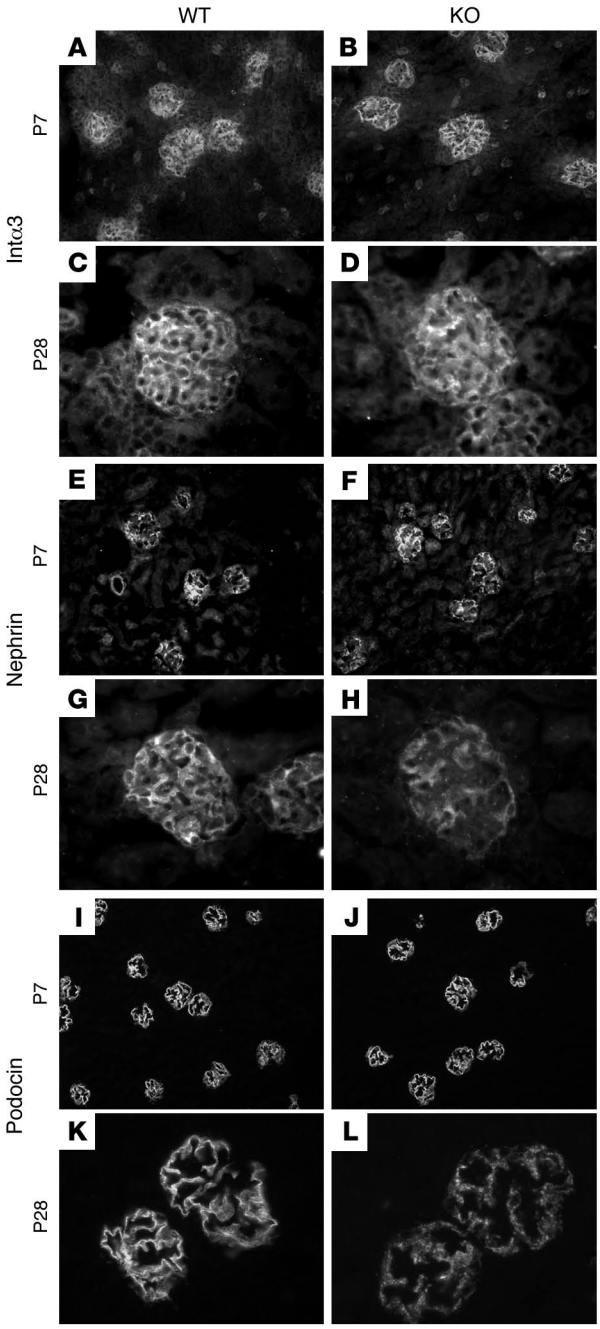

Figure 2
Immunofluorescence detection of podocyte proteins. Frozen sections of normal (left) and *Lamb2*$^{-/-}$ (right) kidneys at P7 and P28 were stained for integrin α3 (Intα3; **A**–**D**), nephrin (**E**–**H**), and podocin (**I**–**L**). There were no detectable changes in intensity or distribution of these proteins in young mice. However, with age and disease progression, there was a reduction in intensity; all 3 seemed to lose their normal linear distribution and showed a more diffuse granular pattern. This likely reflects the retraction of FPs and reduced SD density. Magnification, P7, ×200; P28, ×600.

(16, 17, 20). We also investigated podocyte laminin receptor expression, which is represented primarily by integrin α3β1. Antibody staining for integrin α3 revealed normal distribution and intensity early in the disease process (P7; Figure 2, A and B). In contrast, in older mice (2–4 weeks), there were subtle but clear differences in intensity and distribution. Integrin α3 staining was less intense and lost its typical linear localization (Figure 2, C and D), in parallel to the progressive nephrotic syndrome and FP effacement. In contrast, no changes were detected in integrin α6, integrin α8, or α-dystroglycan localization or expression (data not shown).

Expression of SD components. Currently, the most favored views of the GFB propose the podocyte SD as the predominant determinant, with proteinuria and nephrotic syndrome ensuing upon loss or alteration of SD components or associated proteins (21, 22). We therefore considered the possibility that alterations in the *Lamb2*$^{-/-}$ GBM caused proteinuria indirectly by altering expression or localization of SD components. However, despite congenital albuminuria in *Lamb2*$^{-/-}$ mice (Figure 3A), nephrin (Figure 2, E and F) and podocin (Figure 2, I and J) showed normal distribution and intensity until P14. It was not until after approximately P21 that we were able to detect significant changes in nephrin and podocin levels and distribution (Figure 2, G, H, K, and L), which were comparable to the changes in integrin α3 and likely reflected the widespread FP effacement (9). In addition, we previously reported that CD2AP exhibits an abnormal granular distribution in P21 *Lamb2*$^{-/-}$ podocytes, whereas distribution at P9 was normal (23). These observations suggest that changes in integrin and SD components are unlikely to be the primary cause of proteinuria, but they rather represent secondary changes related to progression of disease caused by the primary GBM defect.

Glomerular features. To further investigate the temporal relationship between podocyte FP effacement and proteinuria, we followed these events chronologically. Increased urinary albumin excretion was detected by SDS-PAGE in *Lamb2*$^{-/-}$ mice as early as P2 (Figure 3, A and D). Kidneys from the same animals were viewed using scanning electron microscopy (SEM). Despite increased albumin excretion, there was no detectable FP effacement (Figure 3, B, C, E, and F). The most distinctive change was mild podocyte cell body villous transformation (Figure 3 and Supplemental Figure 1; supplemental material available online with this article; doi:10.1172/JCI28414DS1), which was detected previously in experimental nephrotic diseases (24). Transmission electron microscopy (TEM) confirmed the presence of normal-appearing SDs and the absence of FP effacement at early ages (Supplemental Figure 2). Segmental podocyte FP effacement was evident at approximately P10 (Figure 3, H and I), whereas the GBM itself generally appeared normal even near the time of death (9), except for occasional, mild, segmental irregularities.

Negative charge characteristics. Although laminins are not considered to be highly charged, they do provide the scaffold for incorporation of BM components that impart anionic charge, such as the sulfated proteoglycans perlecan and agrin. GBM anionic sites revealed by polyethylenimine labeling are normally distributed at regular intervals juxtaposed to podocytes and endothelial cells, but they are sparse in the middle of the GBM (the lamina densa) (25). Charge density on the podocyte aspect is relatively constant throughout life, but charges at the endothelial aspect decrease with age, and in mice they reach a stable number and distribution at 3–4 weeks. Previously it was shown that negative charge distribution and number correlated well with GBM abnormalities in diabetic rats and was disorganized in proteinuric diseases (26). In newborn *Lamb2*$^{-/-}$ mice, the number of anionic sites at the podo-

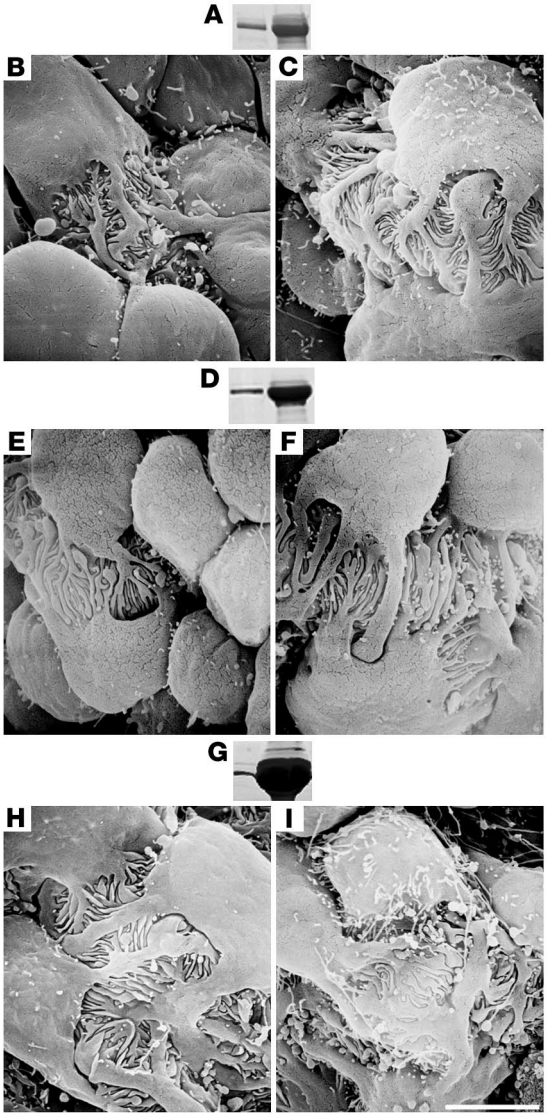

Figure 3
Relationship between proteinuria and FP effacement in *Lamb2*$^{-/-}$ glomeruli. (**A**, **D**, and **G**) Equal volumes of urine from normal (left lanes) and *Lamb2*$^{-/-}$ (right lanes) littermates at P2, P5, and P10 (respectively) were analyzed by SDS-PAGE. Corresponding kidneys from normal (**B**, **E**, and **H**) and *Lamb2*$^{-/-}$ (**C**, **F**, and **I**) mice were analyzed by SEM. At P2 (**B** and **C**) and P5 (**E** and **F**), there were no signs of FP effacement, whereas areas of effacement were evident at P10 (**H** and **I**). Scale bar in **I**: 3 μm.

cyte aspect of the GBM was mildly reduced (Figure 4A), and in general they were less regularly distributed compared with those in control or non-nephrotic *Lamb2*$^{-/-}$NEPH-B2 mice. There was also a slight trend toward more anionic sites in the *Lamb2*$^{-/-}$ lamina densa (Figure 4A). After P14 there was a great increase in the number of anionic sites in the lamina densa, and the mild reduction at the podocyte aspect persisted with age (Figure 4, B–D). Besides these quantitative differences, *Lamb2*$^{-/-}$ charged sites tended to be smaller and irregularly spaced as compared with those in littermate controls, especially in older mice. Thus, the lack of laminin β2 results in disorganization of anionic charges. In the absence of specific methods for probing GBM organization, we propose that these data reflect an overall disorganization of GBM architecture.

Ferritin permeability. To test the consequences of altered GBM composition and organization in *Lamb2*$^{-/-}$ mice, we used native ferritin as a tracer. Ferritin is a large, 480-kDa protein with an iron core containing up to 2,500 iron atoms, making it electron dense. It has been used since the early 1960s to study glomerular permselectivity (27). Ferritin was injected intravenously into control/*Lamb2*$^{-/-}$ littermate pairs at P11–P23 and visualized by TEM. There was a substantial increase in the number of ferritin particles in *Lamb2*$^{-/-}$ versus control GBM as early as 5 minutes after injection (data not shown), and this persisted at later time points. Multiple experiments comparing littermates at 1 (Figure 5A and Supplemental Figure 3) and 2 hours (Figure 5, B–D,

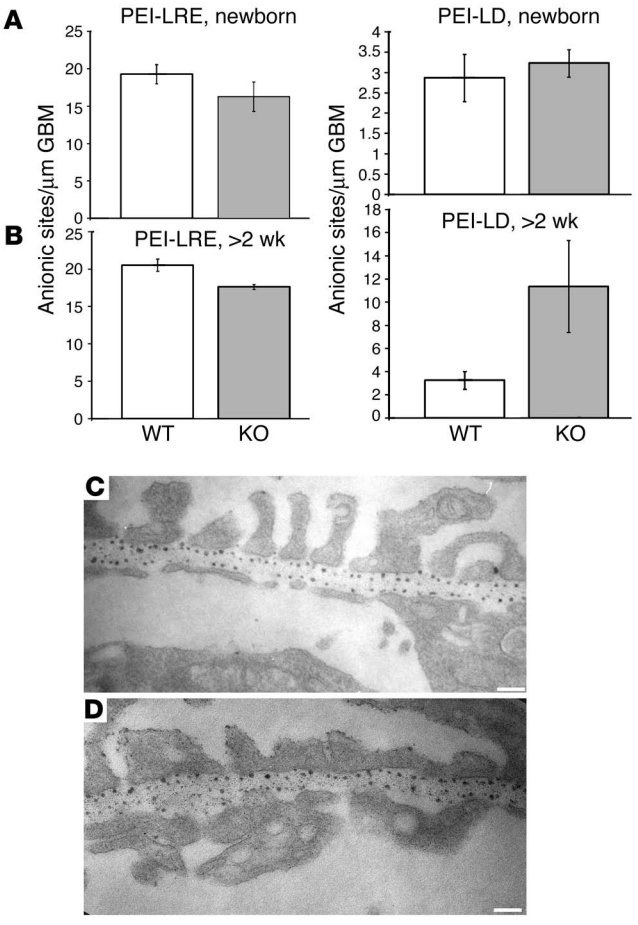

Figure 4
GBM anionic charge distribution. Anionic sites were localized in normal and *Lamb2*$^{-/-}$ glomeruli (as indicated) at birth (**A**) and after 2 weeks of age (**B**–**D**) using polyethylenimine. Anionic sites were counted and expressed as the number of sites/micrometer of GBM length in either the lamina densa (LD; middle of the GBM) or the lamina rara externa (LRE; podocyte aspect). There was a slight but consistent reduction in the total number of LRE anionic sites in the *Lamb2*$^{-/-}$ GBM, but an increase in the number of LD anionic sites at later ages, consistent with GBM disorganization. Data shown in **A** and **B** are mean ± SD. Scale bars: 125 nm.

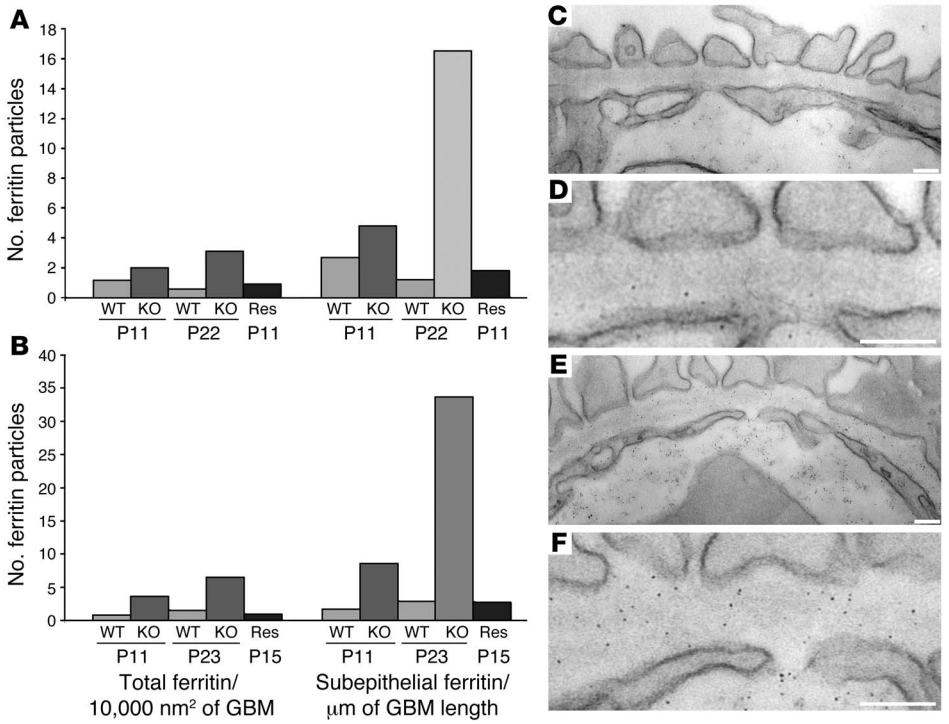

Figure 5
Increased GBM permeability to ferritin in *Lamb2*$^{-/-}$ mice. Ferritin was detected in the GBM either 1 (**A**) or 2 (**B**) hour after a single intravenous injection into control/mutant littermate pairs, at the indicated ages. Ferritin particles were counted in the total surface area of the GBM (expressed as number of ferritin particles/10,000 nm^2) or only at the subepithelial (podocyte) aspect (expressed as number of ferritin particles/μm of GBM length). There was an increase in total and in subepithelial ferritin at 1 hour in all *Lamb2*$^{-/-}$ mice compared with control or non-nephrotic, rescued *Lamb2*$^{-/-}$ mice carrying the NEPH-B2 transgene (Res). The increase was more remarkable after 2 hours in the older mice. (**C**–**F**) Representative electron micrographs showing ferritin particles in the GBM of normal (**C** and **D**) and *Lamb2*$^{-/-}$ (**E** and **F**) mice at P11. Note the increased ferritin in the mutant GBM despite the normal FP architecture. **D** and **F** are higher magnifications of **C** and **E**, respectively. Scale bars: 125 nm.

and Supplemental Figure 4) after injection consistently showed increased ferritin levels in the mutant GBM. The difference was even greater for subepithelial ferritin particles (Figure 5, A and B, and Supplemental Figures 3 and 4). Importantly, the presence or absence of FP effacement did not significantly affect GBM ferritin permeability. Furthermore, ferritin permeability in non-nephrotic *Lamb2*$^{-/-}$ mice carrying the NEPH-B2 transgene was normal (Figure 5, A and B), providing additional evidence that expression of laminin β2 solely by podocytes is sufficient for a normal GFB. Although there was some variability among experiments, this did not alter the overall conclusion; total ferritin numbers were 1.7- to 5.2-fold higher in *Lamb2*$^{-/-}$ GBM, and the subepithelial ferritin was 1.7- to 13.7-fold higher. Thus, the primary GBM defect increased the permeability of the GBM to ferritin independent of detectable podocyte defects.

To assay ferritin permeability in mice with proteinuria due to a primary podocyte defect, we used *Cd2ap*$^{-/-}$ mice. These mutants develop proteinuria during the first 10 days of life and eventually die with nephrotic syndrome and extensive glomerular fibrosis at 7–13 weeks, but GBM composition appears normal (28, 29). GBM ferritin distribution was surprisingly different from that observed in *Lamb2*$^{-/-}$ mice: (a) the total number of GBM ferritin particles was unchanged from control; and (b) there was a trend toward fewer (~70% of control) subepithelial particles in *Cd2ap*$^{-/-}$ GBM, even in areas with extensive FP effacement (Figure 6 and Supplemental Figures 5 and 6). Together, these ferritin studies in 2 distinct models of nephrotic syndrome reveal a clear difference in intrinsic GBM permeability that depends upon and is consistent with the nature of the primary defect.

Discussion

Nephrotic syndrome describes a heterogeneous group of kidney diseases characterized by increased urinary protein (especially albumin), edema, hypoalbuminemia, hyperlipidemia, and lipiduria. Although the definition is clear, and disruption of the GFB is a shared feature, the etiology and rate of progression to renal failure varies. Extensive studies over the last 50 years have attempted to define the role of each of the 3 layers that constitute the GFB in mediating permselectivity, yet controversy still exists. Initially the GBM was viewed as the predominant factor, but recent investigations have revealed strong, direct links between proteinuric disorders of both genetic and idiopathic origins to podocytes and the SD (21, 22, 30, 31).

The availability of animal models provides powerful tools for attempting to distinguish the role of the GBM and SD. Here we have used *Lamb2*$^{-/-}$ and *Cd2ap*$^{-/-}$ mice, 2 distinct models of nephrotic syndrome, to better understand the nature of the GFB. By both following the progression of proteinuria with respect to the timing of podocyte FP effacement and quantitating the entry of an electron-dense tracer molecule into the GFB, we have found strong evidence that the GBM serves as a major barrier to plasma protein that acts independently of the overlying podocyte. Despite ferritin's large size compared with albumin (480 versus 67 kDa), previous localization of albumin in normal rat glomeruli by Ryan and Karnovsky (32) showed a pattern with striking similarity to that of ferritin in our normal mice.

Proteinuria in *Lamb2*$^{-/-}$ mice stems from a primary GBM defect. Laminin β2 is part of LM-521, the predominant laminin in mature GBM. In the absence of laminin β2, and despite compensation by other laminins, the GBM is abnormally organized, as shown by aberrant localization of anionic sites. The abnormal organization could arise in part from the deposition of multiple ectopic laminins (LM-511, -111, -211, and -332) that are not normally found in the GBM but whose presence is expected to change the usual gel properties and overall porosity of the GBM (26). This could lead to the observed increased permeability and exposure of podocytes to atypical hemodynamic forces.

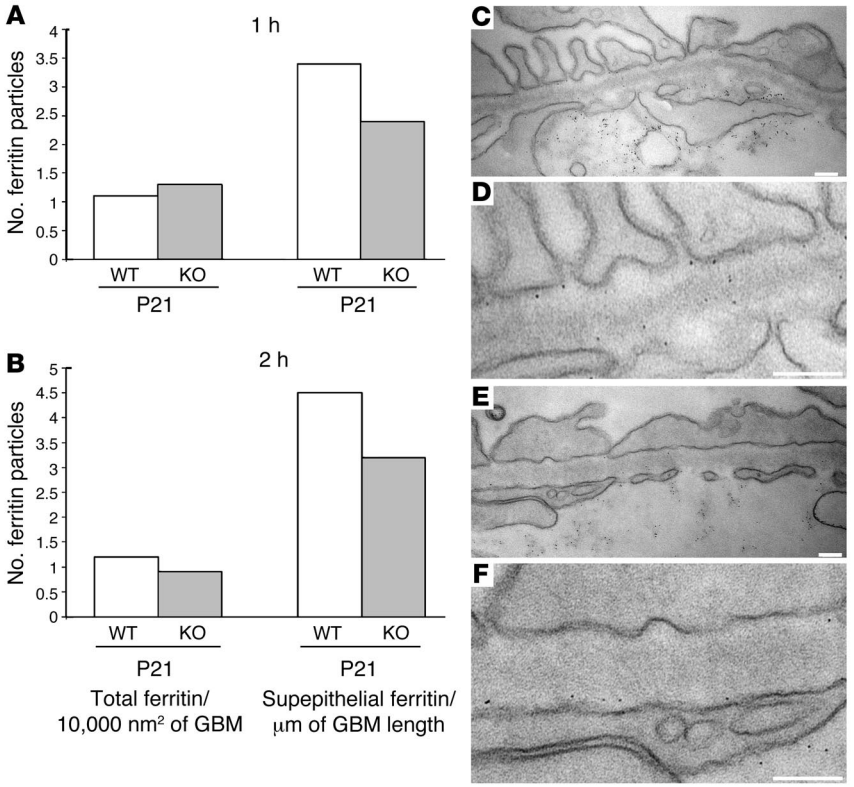

Figure 6
Normal GBM permeability to ferritin in *Cd2ap*$^{-/-}$ mice. Ferritin injections were performed in *Cd2ap*$^{-/-}$ and control littermate mice. (**A** and **B**) Total numbers of ferritin particles in the GBM at 1 and 2 hours after injection were similar in nephrotic *Cd2ap*$^{-/-}$ mice and their normal littermates at P21. However, subepithelial ferritin particle numbers were lower in the mutant, despite the albuminuria. (**C**–**F**) Representative electron micrographs showing ferritin particles in the GBM of P21 normal (**C** and **D**) and *Cd2ap*$^{-/-}$ (**E** and **F**) mice. **D** and **F** are higher magnifications of **C** and **E**, respectively. Scale bars: 125 nm.

We also examined podocyte architecture early during disease course and defined its relationship to proteinuria. During the first week of life, proteinuric *Lamb2*$^{-/-}$ mice had apparently normal FPs and SDs, and it was not until the second week that there was gradual FP effacement and loss of SDs. Thus, increased urinary protein clearly preceded detectable podocyte FP and SD changes. Proteinuria in the absence of widespread FP effacement indicates that the SD, which appears intact in young *Lamb2*$^{-/-}$ mice, is not a wholly effective barrier to albumin, a conclusion also reached in rat studies (33). However, here we cannot rule out the possibility that the observed SDs are defective. We note that we are not the first to report the existence of proteinuria in the absence of FP effacement; it has also been observed in preeclampsia, in other animal models, and in sporadic human cases (34–38).

In contrast to our findings in *Lamb2*$^{-/-}$ mice, entry of ferritin into the GBM was near normal in heavily proteinuric *Cd2ap*$^{-/-}$ mice, which have a primary podocyte defect and a compositionally normal GBM (28, 29). This shows that not all nephrotic mice exhibit GBM ferritin permeability changes, and it provides further support for the notion that the GBM is the primary sieve and acts as a modified gel, in accord with the gel permeation/diffusion hypothesis (15). This hypothesis introduced the idea that the mechanism of proteinuria varies depending on the site of the primary defect (GBM or podocyte). The hypothesis predicts that only slightly fewer macromolecules will cross the normal GBM in the presence of FP effacement, but the accompanying reduced hydraulic permeability (12, 39) of the GFB (i.e., reduced single-nephron GFR) will lead to a decreased dilution factor and a greatly increased concentration of macromolecules in the glomerular filtrate. This is in contrast to an abnormal GBM, where there is a simple increased flux of macromolecules. In both cases, the proximal tubule's protein reabsorption machinery would then be unable to handle this increased concentration, resulting in proteinuria (15).

So what causes the eventual FP effacement in *Lamb2*$^{-/-}$ mice? In vitro studies suggest that albumin and IgG at plasma concentrations stimulate changes in the podocyte cytoskeleton that could cause or be indicative of podocyte damage (40). Although in culture the exposure affects the apical surface, multiple observations have suggested that podocytes can exhibit high endocytic activity at the basolateral surface in vivo, especially in nephrotic conditions (27, 41–44). Thus, there may be a tremendous advantage to sheltering podocytes from high plasma protein concentrations, which in turn underscores the central importance of the GBM in serving as the major component of the GFB.

One important outcome of these studies is that we have been able to show in situ that the GFB is differentially affected in 2 genetically defined proteinuric diseases, reinforcing the notion that high-level proteinuria can reflect different mechanistic paths. It is also notable that nephrin, podocin, CD2AP, and integrin α3 were localized normally until the second week despite the proteinuria in *Lamb2*$^{-/-}$ mice, consistent with normal podocyte architecture, but eventually their intensity and distribution changed markedly. Given that these abnormalities are far removed from the primary insult that causes proteinuria (i.e., lack of laminin β2), caution should be used in drawing conclusions from similar analysis of human biopsy samples, as they are invariably taken late during the course of disease.

Methods

Animal models. *Lamb2*$^{-/-}$ mice and podocyte- and muscle-specific transgenic rescue of *Lamb2*$^{-/-}$ phenotypes have been described (7–9), as have *Cd2ap*$^{-/-}$ mice (28). *Lamb2*$^{-/-}$MCK-B2 (muscle-rescued) mice were used as mutants for most experiments; in a few cases, *Lamb2*$^{-/-}$ mice younger than P12 without the transgene were used. For simplicity, all mutants are designated *Lamb2*$^{-/-}$, indicating glomerular genotype. Control/mutant pairs were taken from the same litter. All procedures and experiments were approved by the Washington University Animal Studies Committee.

Urinalysis. Equal volumes of urine (15 μl) were analyzed on precast 4–20% SDS polyacrylamide gels (Invitrogen), which were stained with Coomassie blue. For quantitation, protein and creatinine concentrations were measured with a COBAS MIRA plus analyzer (Roche Diagnostics).

Light and electron microscopy. Kidneys were fixed in 10% buffered formalin, embedded in paraffin, sectioned, and stained with H&E and PAS by standard methods. For TEM, tissues were fixed, embedded in plastic, sectioned, and stained as previously described (8). For SEM, small pieces (approximately 2-mm cubes) of kidney cortex were fixed in 3% phosphate-buffered glutaraldehyde and postfixed in 1% phosphate-buffered osmium tetroxide. Samples were dehydrated in graded ethanols and critical-point dried in carbon dioxide. The cubes were then cracked into pieces by stressing with the edge of a razor blade and mounted with glue onto stubs. The surface was sputter-coated using gold/palladium and visualized by SEM.

Antibodies and immunofluorescence. Rabbit anti-mouse laminin α5 serum was described previously (45). Rat anti-mouse laminin α2 mAb 4H8-2 was purchased from ALEXIS Biochemicals (Axxora). Other primary antibodies were gifts from generous colleagues: rabbit anti-mouse laminin β2 (46) from Takako Sasaki and Rupert Timpl, Max Planck Institute for Biochemistry, Martinsried, Germany; rat anti-mouse laminin α1 mAb 8B3 (47) from Dale Abrahamson, University of Kansas Medical Center, Kansas City, Kansas, USA; rabbit anti-human laminin-332 (α3β3γ2) (48) from Peter Marinkovich, Stanford University, Stanford, California, USA; rabbit anti-chick integrin α3 (49) from Mike Dipersio, Albany Medical College, Albany, New York, USA; rabbit anti-mouse nephrin (50) from Lawrence Holzman, University of Michigan, Ann Arbor, Michigan, USA; rabbit anti-human podocin (51) from Corinne Antignac, Necker Hospital, Paris. Alexa 488- and Cy3-conjugated secondary antibodies were purchased from Invitrogen and Chemicon International, respectively. Immunofluorescence analysis was performed as previously described (9).

Negative charge detection. Using a method modified from ref. 52, small kidney cortex pieces were incubated in 0.5% polyethylenimine (1.8 kDa; Sigma-Aldrich), pH 7.3, for 30 minutes on ice, washed, and fixed in 2.5% glutaraldehyde containing 2% phosphotungstic acid for 1 hour on ice. After washing, tissues were postfixed in 1% osmium tetroxide for 2 hours at 4°C. Samples were then dehydrated and embedded in plastic. Ultrathin sections were viewed by TEM without staining. Three to 4 glomeruli were visualized for each condition, with a minimum of 8 individual loops photographed. Ten mice at P0 (4 mutant and 6 control) and 9 in the older group (4 mutant and 5 control) were assayed. To reveal abnormalities in the distribution of GBM anionic sites, the numbers of polyethylenimine-positive sites in the lamina densa and lamina rara externa were determined using high-resolution images. GBM length was calculated using SPOT 4.0.1 software (Diagnostic Instruments). Data are mean ± SD.

Ferritin permselectivity. Using methods modified from Farquhar (27), horse spleen ferritin (50 mg/ml in 0.9% NaCl) was administered via tail vein injection at 10 μl/g body weight. After various times (5 minutes to 2 hours), kidneys were fixed in situ by injecting fixative (4% paraformaldehyde, 4% glutaraldehyde) beneath the capsule. After 5 minutes kidneys were cut into small pieces that were further fixed in 1% paraformaldehyde, 1% glutaraldehyde overnight and postfixed in 1.5% potassium ferrocyanide, 1% osmium tetroxide. Specimens were dehydrated, embedded in plastic, sectioned, and visualized by TEM unstained. To quantify GBM permeability, electron-dense ferritin particles in the GBM were counted using high-resolution images. Total GBM surface area and length were calculated using SPOT software (Diagnostic Instruments). Ferritin numbers were expressed as total/10,000 nm^2 of GBM surface area and subepithelial ferritin/micrometer GBM length. Subepithelial refers to the distal third of the GBM, nearest the FPs.

Acknowledgments

We thank Peter Marinkovich, Dale Abrahamson, Takako Sasaki, Rupert Timpl, Larry Holzman, Corinne Antignac, and Mike Dipersio for antibodies; Patricia St. John for advice on visualizing ferritin; Dan Martin, Marilyn Levy, Mike Veith, Jennifer Richardson, and the Mouse Genetics Core for assistance; and Scott Harvey and John Sedor for comments on the manuscript. This work was funded by grants from the NIH (R01DK064687 and R01GM060432), an Established Investigator Award from the American Heart Association to J.H. Miner, and a Research Grant from the National Kidney Foundation of Eastern Missouri and Metro East to G. Jarad. Mice were housed in a facility supported by NIH grant C06RR015502.

Received for publication March 6, 2006, and accepted in revised form May 16, 2006.

Address correspondence to: Jeffrey H. Miner, Washington University School of Medicine, Renal Division, Box 8126, 660 South Euclid Avenue, St. Louis, Missouri 63110, USA. Phone: (314) 362-8235; Fax: (314) 362-8237; E-mail: minerj@wustl.edu.

Portions of this work were presented at the 2005 Annual Meeting of the American Society of Nephrology in Philadelphia, Pennsylvania, USA, on November 11, 2005.

1. Miner, J.H., and Yurchenco, P.D. 2004. Laminin functions in tissue morphogenesis. *Annu. Rev. Cell Dev. Biol.* **20**:255–284.
2. Sasaki, T., Fassler, R., and Hohenester, E. 2004. Laminin: the crux of basement membrane assembly. *J. Cell Biol.* **164**:959–963.
3. Miner, J.H. 1999. Renal basement membrane components. *Kidney Int.* **56**:2016–2024.
4. Abrahamson, D.R. 1985. Origin of the glomerular basement membrane visualized after in vivo labeling of laminin in newborn rat kidneys. *J. Cell Biol.* **100**:1988–2000.
5. Aumailley, M., et al. 2005. A simplified laminin nomenclature. *Matrix Biol.* **24**:326–332.
6. Miner, J.H., and Li, C. 2000. Defective glomerulogenesis in the absence of laminin α5 demonstrates a developmental role for the kidney glomerular basement membrane. *Dev. Biol.* **217**:278–289.
7. Noakes, P.G., Gautam, M., Mudd, J., Sanes, J.R., and Merlie, J.P. 1995. Aberrant differentiation of neuromuscular junctions in mice lacking s-laminin/laminin β2. *Nature.* **374**:258–262.
8. Noakes, P.G., et al. 1995. The renal glomerulus of mice lacking s-laminin/laminin β2: nephrosis despite molecular compensation by laminin β1. *Nat. Genet.* **10**:400–406.
9. Miner, J.H., Go, G., Cunningham, J., Patton, B.L., and Jarad, G. 2006. Transgenic isolation of skeletal muscle and kidney defects in laminin beta2 mutant mice: implications for Pierson syndrome. *Development.* **133**:967–975.
10. Zenker, M., et al. 2004. Human laminin beta2 deficiency causes congenital nephrosis with mesangial sclerosis and distinct eye abnormalities. *Hum. Mol. Genet.* **13**:2625–2632.
11. Deen, W.M. 2004. What determines glomerular capillary permeability? *J. Clin. Invest.* **114**:1412–1414. doi:10.1172/JCI200423577.
12. Deen, W.M., Lazzara, M.J., and Myers, B.D. 2001. Structural determinants of glomerular permeability. *Am. J. Physiol. Renal Physiol.* **281**:F579–F596.
13. Whiteside, C.I., Cameron, R., Munk, S., and Levy, J. 1993. Podocytic cytoskeletal disaggregation and basement-membrane detachment in puromycin aminonucleoside nephrosis. *Am. J. Pathol.* **142**:1641–1653.
14. Yu, D., et al. 2005. Urinary podocyte loss is a more specific marker of ongoing glomerular damage than proteinuria. *J. Am. Soc. Nephrol.* **16**:1733–1741.
15. Smithies, O. 2003. Why the kidney glomerulus does not clog: a gel permeation/diffusion hypothesis of renal function. *Proc. Natl. Acad. Sci. U. S. A.* **100**:4108–4113.
16. Kashtan, C.E., et al. 2001. Abnormal glomerular basement membrane laminins in murine, canine and human Alport syndrome: aberrant laminin alpha2 deposition is species-independent. *J. Am. Soc. Nephrol.* **12**:252–260.
17. Cosgrove, D., et al. 2000. Integrin alpha1beta1 and transforming growth factor-beta1 play distinct roles in Alport glomerular pathogenesis and serve as dual targets for metabolic therapy. *Am. J. Pathol.* **157**:1649–1659.
18. Park, C.H., and Maack, T. 1984. Albumin absorption and catabolism by isolated perfused proximal convoluted tubules of the rabbit. *J. Clin. Invest.* **73**:767–777.
19. Miner, J.H. 2005. Building the glomerulus: a matricentric view. *J. Am. Soc. Nephrol.* **16**:857–861.
20. Abrahamson, D.R., Prettyman, A.C., Robert, B., and St. John, P.L. 2003. Laminin-1 reexpression in Alport mouse glomerular basement membranes. *Kidney Int.* **63**:826–834.
21. Kerjaschki, D. 2001. Caught flat-footed: podocyte damage and the molecular bases of focal

glomerulosclerosis. *J. Clin. Invest.* **108**:1583–1587. doi:10.1172/JCI200114629.
22. Wartiovaara, J., et al. 2004. Nephrin strands contribute to a porous slit diaphragm scaffold as revealed by electron tomography. *J. Clin. Invest.* **114**:1475–1483. doi:10.1172/JCI200422562.
23. Li, C., Ruotsalainen, V., Tryggvason, K., Shaw, A.S., and Miner, J.H. 2000. CD2AP is expressed with nephrin in developing podocytes and is found widely in mature kidney and elsewhere. *Am. J. Physiol. Renal Physiol.* **279**:F785–F792.
24. Andrews, P.M. 1977. A scanning and transmission electron microscopic comparison of puromycin aminonucleoside-induced nephrosis to hyperalbuminemia-induced proteinuria with emphasis on kidney podocyte pedicel loss. *Lab. Invest.* **36**:183–197.
25. Kanwar, Y.S., and Farquhar, M.G. 1979. Anionic sites in the glomerular basement membrane. In vivo and in vitro localization to the laminae rarae by cationic probes. *J. Cell Biol.* **81**:137–153.
26. Isogai, S., Mogami, K., Ouchi, H., and Yoshino, G. 2000. An impairment of barrier size and charge selectivity of glomerular basement membrane in streptozotocin-induced diabetes and prevention by pharmacological therapy. *Med. Electron Microsc.* **33**:123–129.
27. Farquhar, M.G., Wissig, S.L., and Palade, G.E. 1961. Glomerular permeability. I. Ferritin transfer across the normal glomerular capillary wall. *J. Exp. Med.* **113**:47–66.
28. Shih, N.-Y., et al. 1999. Congenital nephrotic syndrome in mice lacking CD2-associated protein. *Science.* **286**:312–315.
29. Grunkemeyer, J.A., Kwoh, C., Huber, T.B., and Shaw, A.S. 2005. CD2-associated protein (CD2AP) expression in podocytes rescues lethality of CD2AP deficiency. *J. Biol. Chem.* **280**:29677–29681.
30. Tryggvason, K., and Wartiovaara, J. 2001. Molecular basis of glomerular permselectivity. *Curr. Opin. Nephrol. Hypertens.* **10**:543–549.
31. Pavenstadt, H., Kriz, W., and Kretzler, M. 2003. Cell biology of the glomerular podocyte. *Physiol. Rev.* **83**:253–307.
32. Ryan, G.B., and Karnovsky, M.J. 1976. Distribution of endogenous albumin in the rat glomerulus: role of hemodynamic factors in glomerular barrier function. *Kidney Int.* **9**:36–45.
33. Lund, U., et al. 2003. Glomerular filtration rate dependence of sieving of albumin and some neutral proteins in rat kidneys. *Am. J. Physiol. Renal Physiol.* **284**:F1226–F1234.
34. Karumanchi, S.A., Epstein, F.H., and Stillman, I.E. 2005. Is loss of podocyte foot processes necessary for the induction of proteinuria? [letter]. *Am. J. Kidney Dis.* **45**:436.
35. D'Amico, G., and Bazzi, C. 2003. Pathophysiology of proteinuria. *Kidney Int.* **63**:809–825.
36. Good, K.S., O'Brien, K., Schulman, G., Kerjaschki, D., and Fogo, A.B. 2004. Unexplained nephrotic-range proteinuria in a 38-year-old man: a case of "no change disease." *Am. J. Kidney Dis.* **43**:933–938.
37. Liu, G., et al. 2003. Neph1 and nephrin interaction in the slit diaphragm is an important determinant of glomerular permeability. *J. Clin. Invest.* **112**:209–221. doi:10.1172/JCI200318242.
38. Orikasa, M., Matsui, K., Oite, T., and Shimizu, F. 1988. Massive proteinuria induced in rats by a single intravenous injection of a monoclonal antibody. *J. Immunol.* **141**:807–814.
39. Bohman, S.O., Jaremko, G., Bohlin, A.B., and Berg, U. 1984. Foot process fusion and glomerular filtration rate in minimal change nephrotic syndrome. *Kidney Int.* **25**:696–700.
40. Morigi, M., et al. 2005. In response to protein load podocytes reorganize cytoskeleton and modulate endothelin-1 gene: implication for permselective dysfunction of chronic nephropathies. *Am. J. Pathol.* **166**:1309–1320.
41. Farquhar, M.G., and Palade, G.E. 1961. Glomerular permeability. II. Ferritin transfer across the glomerular capillary wall in nephrotic rats. *J. Exp. Med.* **114**:699–716.
42. Farquhar, M.G., and Palade, G.E. 1960. Segregation of ferritin in glomerular protein absorption droplets. *J. Biophys. Biochem. Cytol.* **7**:297–304.
43. Vogt, A., Bockhorn, H., Kozima, K., and Sasaki, M. 1968. Electron microscopic localization of the nephrotoxic antibody in the glomeruli of the rat after intravenous application of purified nephritogenic antibody-ferritin conjugates. *J. Exp. Med.* **127**:867–878.
44. Ina, K., Kitamura, H., Tatsukawa, S., Takayama, T., and Fujikura, Y. 2002. Glomerular podocyte endocytosis of the diabetic rat. *J. Electron Microsc. (Tokyo).* **51**:275–279.
45. Miner, J.H., et al. 1997. The laminin alpha chains: expression, developmental transitions, and chromosomal locations of alpha1-5, identification of heterotrimeric laminins 8-11, and cloning of a novel alpha3 isoform. *J. Cell Biol.* **137**:685–701.
46. Sasaki, T., Mann, K., Miner, J.H., Miosge, N., and Timpl, R. 2002. Domain IV of mouse laminin β1 and β2 chains: structure, glycosaminoglycan modification and immunochemical analysis of tissue contents. *Eur. J. Biochem.* **269**:431–442.
47. St. John, P.L., et al. 2001. Glomerular laminin isoform transitions: errors in metanephric culture are corrected by grafting. *Am. J. Physiol. Renal Physiol.* **280**:F695–F705.
48. Marinkovich, M.P., Lunstrum, G.P., and Burgeson, R.E. 1992. The anchoring filament protein kalinin is synthesized and secreted as a high molecular weight precursor. *J. Biol. Chem.* **267**:17900–17906.
49. DiPersio, C.M., Shah, S., and Hynes, R.O. 1995. Alpha 3A beta 1 integrin localizes to focal contacts in response to diverse extracellular matrix proteins. *J. Cell Sci.* **108**:2321–2336.
50. Holzman, L.B., et al. 1999. Nephrin localizes to the slit pore of the glomerular epithelial cell. *Kidney Int.* **56**:1481–1491.
51. Roselli, S., et al. 2002. Podocin localizes in the kidney to the slit diaphragm area. *Am. J. Pathol.* **160**:131–139.
52. Isogai, S., Mogami, K., Shiina, N., and Yoshino, G. 1999. Initial ultrastructural changes in pore size and anionic sites of the glomerular basement membrane in streptozotocin-induced diabetic rats and their prevention by insulin treatment. *Nephron.* **83**:53–58.